Changes in the surface energy budget after fire in boreal ecosystems of interior Alaska: An annual perspective

Heping Liu,[1,2] James T. Randerson,[3] Jamie Lindfors,[1] and F. Stuart Chapin III[4]

Received 23 June 2004; revised 28 January 2005; accepted 25 February 2005; published 1 July 2005.

[1] Understanding links between the disturbance regime and regional climate in boreal regions requires observations of the surface energy budget from ecosystems in various stages of secondary succession. While several studies have characterized fire-induced differences in surface energy fluxes from boreal ecosystems during summer months, much less is known about these differences over the full annual cycle. Here we measured components of the surface energy budget (including both radiative and turbulent fluxes) at three sites from a fire chronosequence in interior Alaska for a 1-year period. Our sites consisted of large burn scars resulting from fires in 1999, 1987, and ~1920 (hereinafter referred to as the 3-, 15-, and 80-year sites, respectively). Vegetation cover consisted primarily of bunch grasses at the 3-year site, aspen and willow at the 15-year site, and black spruce at the 80-year site. Annual net radiation declined by 31% (17 W m^{-2}) for both the 3- and the 15-year sites as compared with the 80-year site (which had an annual mean of 55 W m^{-2}). Annual sensible heat fluxes were reduced by an even greater amount, by 55% at the 3-year site and by 52% at the 15-year site as compared with the 80-year site (which had an annual mean of 21 W m^{-2}). Absolute differences between the postfire ecosystems and the mature black spruce forest for both net radiation and sensible heat fluxes were greatest during spring (because of differences in snow cover and surface albedo), substantial during summer and winter, and relatively small during fall. Fire-induced disturbance also initially reduced annual evapotranspiration (ET). Annual ET decreased by 33% (99 mm yr^{-1}) at the 3-year site as compared with the 80-year site (which had an annual flux of 301 mm yr^{-1}). Annual ET at the 15-year site (283 mm yr^{-1}) was approximately the same as that from the 80-year site, even though the 15-year site had substantially higher ET during July. Our study suggests that differences in annual ET between deciduous and conifer stands may be smaller than that inferred solely from summer observations. This study provides a direct means to validate land surface processes in global climate models attempting to capture vegetation-climate feedbacks in northern terrestrial regions.

Citation: Liu, H., J. T. Randerson, J. Lindfors, and F. S. Chapin III (2005), Changes in the surface energy budget after fire in boreal ecosystems of interior Alaska: An annual perspective, *J. Geophys. Res.*, *110*, D13101, doi:10.1029/2004JD005158.

1. Introduction

[2] Interactions between vegetation and the atmosphere have the potential to amplify or to dampen changes in climate caused by other mechanisms, such as contemporary increases in greenhouse gases or longer-term changes in the Earth's orbit. In northern high-latitude regions a defining characteristic of tree species in mature boreal forest ecosystems is that they protrude above the snowpack and thus substantially decrease albedo [*Betts and Ball*, 1997] and increase sensible heat fluxes [*Bonan et al.*, 1995] during winter and spring in contrast with tundra vegetation that often remains buried beneath snow. Consequently, the replacement of boreal forest by tundra in climate models leads to reduced atmospheric heating, cooler air temperatures, and subsequent increases in snow and ice cover [*Bonan et al.*, 1992; *Thomas and Rowntree*, 1992; *Bonan et al.*, 1995].

[3] Several studies present evidence that during the Pleistocene these interactions may have contributed substantially to millennial-scale variability in regional and global climate. For example, although orbital changes may have initiated high-latitude warming during the mid-Holocene (~6000 years ago), the observed northern expansion of boreal forests during this time substantially amplified this warming and contributed approximately half

[1]Division of Geological and Planetary Sciences, California Institute of Technology, Pasadena, California, USA.
[2]Now at Department of Physics, Atmospheric Sciences and General Science, Jackson State University, Jackson, Mississippi, USA.
[3]Department of Earth System Science, University of California, Irvine, California, USA.
[4]Institute of Arctic Biology, University of Alaska Fairbanks, Fairbanks, Alaska, USA.

0148-0227/05/2004JD005158$09.00

of the total increase in surface air temperatures [*Foley et al.*, 1994]. Similarly, a contraction of the boreal biome enhanced orbitally induced cooling ~115,000 years ago and contributed to the onset of the last glaciation [*Gallimore and Kutzbach*, 1996]. Despite the importance of these vegetation feedbacks for climate few observations have been made of the surface energy budget from tundra and boreal forest ecosystems during periods outside the growing season, when vegetation-driven differences in surface albedo are largest [e.g., *Harding and Pomeroy*, 1996; *Eugster et al.*, 2000]. Observations from these periods have the potential to improve our understanding of the basic biophysical and biogeochemical processes that are linked with vegetation cover and may provide a basis for more accurately representing these processes in models used to predict past, contemporary, or future changes in climate [e.g., *Viterbo and Betts*, 1999].

[4] In addition to changes in location of the transition zone between boreal and tundra biomes, vegetation feedbacks to climate change may occur because of shifts in plant functional types within boreal [*Chapin et al.*, 2000; *Eugster et al.*, 2000; *Chambers and Chapin*, 2002] or tundra biomes [*Eaton et al.*, 2001; *Sturm et al.*, 2001; *Liston et al.*, 2002]. In boreal regions of North America, for example, fires often cause stand-replacing mortality that subsequently causes changes in species composition and ecosystem structure. These changes, in turn, affect energy exchange processes for many decades after the initial fire disturbance. Syntheses of observations from multiple field sites provide evidence that during summer months, fire-induced changes in the surface energy budget are comparable to or even larger than differences between mature boreal forest and tundra ecosystems [*Chapin et al.*, 2000; *Eugster et al.*, 2000].

[5] In the earliest stages of secondary succession in boreal ecosystems, grasses and small shrubs remain buried beneath the snowpack during fall, winter, and spring, leading to high albedo values [*Betts and Ball*, 1997] whereas during the summer, black carbon on exposed soil surfaces decreases albedo to values below those typically found in mature conifer stands [*Amiro et al.*, 1999; *Chambers and Chapin*, 2002]. The lower summer albedo and reduced radiation interception by the canopy overstory recovering from fire substantially increases ground heat fluxes [*Amiro*, 2001] and consequently late summer soil active layer depths in areas underlain with permafrost. Even though summer albedo is reduced immediately following fire disturbance for a period of 1–2 years, net radiation remains constant or decreases during summer months (as compared with mature conifer stands) because of the concurrent loss of canopy structure that decreases surface roughness and thus increases surface temperatures and longwave radiation losses [*Chambers and Chapin*, 2002; *Chambers et al.*, 2005]. As a result of these changes both sensible and latent heat fluxes tend to be lower in recent burns during summer months than in nearby mature conifer forests [*Amiro*, 2001; *Chambers and Chapin*, 2002].

[6] In intermediate stages of succession that often persist for many decades, fast growing deciduous shrubs and trees (such as *Salix* and *Populus*) frequently establish and make dominant contributions to surface energy and carbon fluxes [e.g., *Van Cleve et al.*, 1996]. During periods with snow cover these intermediate stages of regrowth also have intermediate values of albedo as compared with early and late successional vegetation [*Betts and Ball*, 1997; *Ohta et al.*, 1999]. During summer, albedo in deciduous forests is often much higher than in nearby conifer ecosystems, with values ranging between 0.13 and 0.18 [*Betts and Ball*, 1997; *Chambers and Chapin*, 2002]. Canopy conductance and evapotranspiration (ET) rates are also high and are often much greater than in nearby mature conifer stands [*Baldocchi et al.*, 2000; *Blanken et al.*, 2001]. This leads to a greater partitioning of net radiation into latent heat and a concurrent decline in sensible heat (i.e., a decrease in the Bowen ratio).

[7] These fire-induced changes in vegetation cover influence biosphere-atmosphere energy exchange at regional and continental scales because fire is an important ecosystem process within both Eurasian and North American boreal regions [*Kasischke and Stocks*, 2000; *Amiro*, 2001; *Conard et al.*, 2002; *Stocks et al.*, 2002]. With increasing fire frequency that may occur in northern ecosystems as a result of warming [*Kasischke et al.*, 1995; *Kasischke and Stocks*, 2000], the extent of areas with low sensible heat fluxes may become larger at regional scales and exert a negative feedback to future warming [*Chapin et al.*, 2000; *Eugster et al.*, 2000; *Chambers and Chapin*, 2002]. The net effect of fire on high-latitude climate remains uncertain, in part, because changes in the surface energy budget outside the growing season have not been quantified and also because other processes and feedbacks are likely to occur simultaneously.

[8] In contrast with the cooling feedback caused by changes in vegetation composition and structure in postfire ecosystems, positive feedbacks from increased fire activity may occur via increased emissions of greenhouse gases that contribute to global warming [*Flannigan and Van Wagner*, 1991; *Kasischke et al.*, 1995; *Kasischke and Stocks*, 2000] or by the release of soot from fire emissions that lowers albedo on glaciers, sea ice, and the Greenland ice sheet [*Hansen and Nazarenko*, 2004]. Multiple records suggest that the growing season has lengthened in northern regions in recent decades [*Serreze et al.*, 2000], and this could, in principle, lead to a longer fire season. It remains a challenge, however, to link recent increases in fire emissions to increased frequency of drought or other meteorological trends [*Girardin et al.*, 2004], even though some of the links between fire activity and synoptic weather events are known [*Skinner et al.*, 2002].

[9] Here we provide measurements of surface energy fluxes over a 1-year period (from 10 April 2002 through 9 April 2003) from three boreal forest ecosystems that are part of a fire chronosequence in interior Alaska. All three sites are located near Delta Junction, Alaska, and experience similar climate. Past work on this chronosequence has examined soil respiration dynamics [*O'Neill et al.*, 2003], microbial diversity [*Treseder et al.*, 2004], remote sensing analyses of burn severity and carbon emissions [*Michalek et al.*, 2000; *French*, 2002], and brief measurements of summer energy exchange [*Chambers and Chapin*, 2002]. One site served as a control and was located in a mature black spruce (*Picea mariana*) forest, while the other two represented early and early/intermediate stages of succession. Our objective is to characterize changes in the annual surface energy budget caused by fire-induced disturbance. A key finding from our analysis is that site level differences

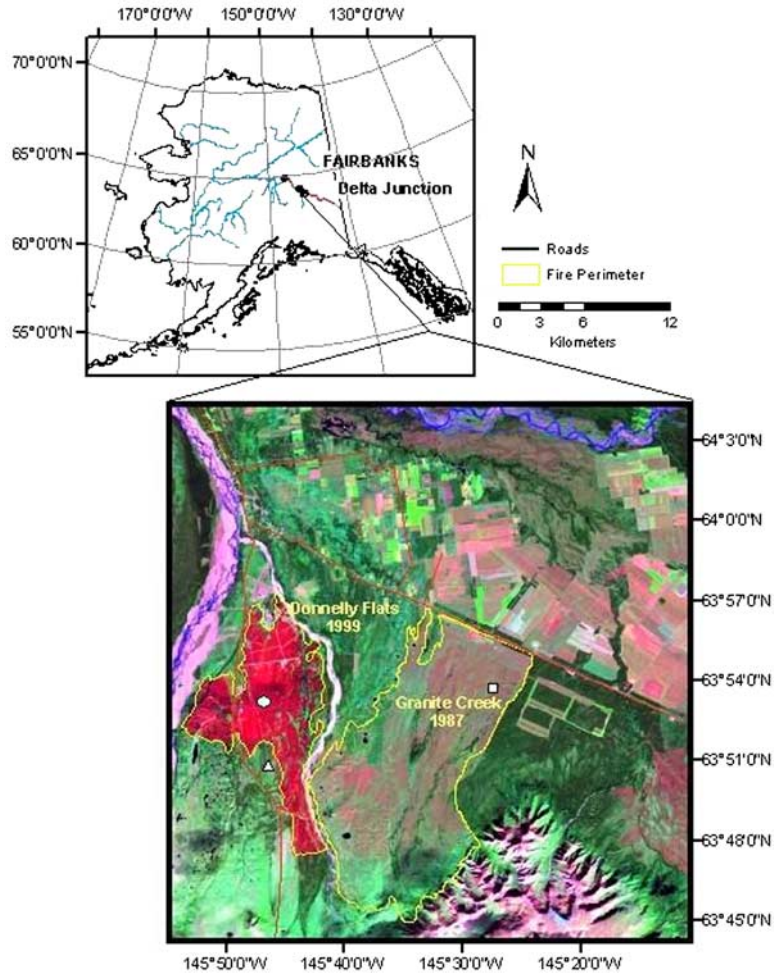

Figure 1. Map of Alaska and a Landsat Enhanced Thematic Mapper Plus (ETM+) satellite image from 10 September 1999 showing the location of our study sites near Delta Junction, Alaska. The Donnelly Flats fire that burned 7.6×10^3 ha in June of 1999 is visible within this false color image as shades of bright red. Our 3-year site was located within the perimeter of this burn (denoted by a circle). The Granite Creek fire that burned 2.0×10^4 ha in 1987 is located directly east of the Donnelly Flats fire and is visible within the image as shades of light red. Our 15-year site was located within the perimeter of this burn (denoted by a square). The 80-year control site was located in unburned black spruce forest directly south of the 3-year site (denoted by a triangle). Agricultural fields near the town of Delta Junction are visible in the northern part of the image, and the Alaska Range is visible in the southern part. This image was provided courtesy of N. French.

in the energy budget were largest during spring as a result of differences in snow cover and surface reflectance.

2. Site Description

[10] This study was conducted near Delta Junction in interior Alaska (63°54′N, 145°40′W) (Figure 1). Interior Alaska experiences a continental climate, characterized by large daily and annual temperature ranges, low humidity, and relatively low precipitation (Western Regional Climate Center (WRCC), station observations available from Big Delta, Alaska, available at http://www.wrcc.dri.edu/climsum.html). For the 30-year period from 1961 to 1990, air temperatures remained above freezing for an average of 141 days, extending from early May to late September. Mean air temperatures were −1.0°C during spring (March, April, and May), 14.2°C during summer (June, July, and August), −4.0°C during fall (September, October, and November), −18.4°C during winter (December, January, and February), and −2.3°C during the full year. Mean precipitation was 12 mm $month^{-1}$ during spring, 61 mm $month^{-1}$ during summer, 19 mm $month^{-1}$ during fall, 8 mm $month^{-1}$ during winter, and 304 mm yr^{-1}. This precipitation included, on average, 940 mm of snowfall (WRCC). The snow was quite dry with 10 mm of snow melting down to less than 1 mm of water (WRCC).

[11] Three sites were selected in ecosystems that were in various stages of recovery following fires that occurred in

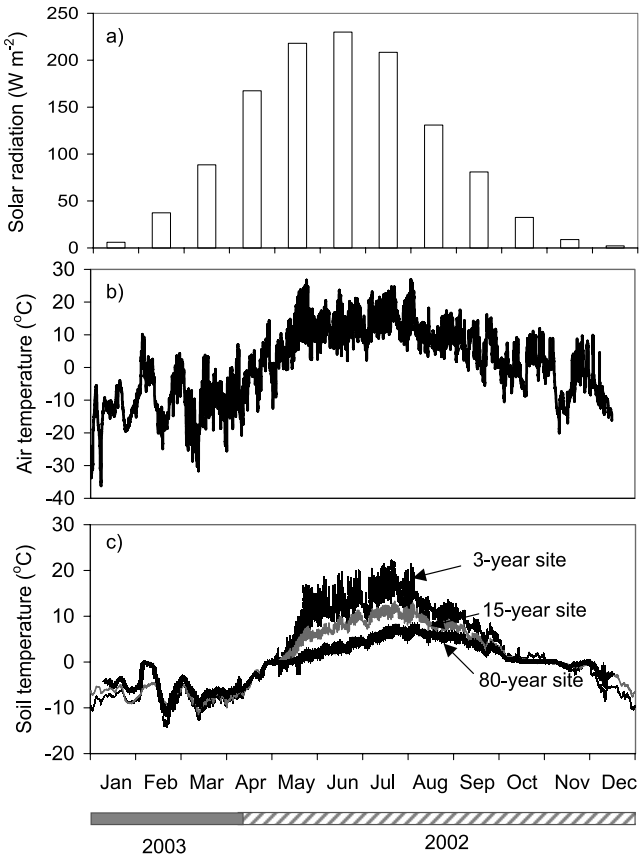

Figure 2. Seasonal patterns of (a) monthly solar radiation, (b) hourly above-canopy air temperature, and (c) hourly soil temperatures at a depth of 10 cm at the three study sites. The solar radiation fluxes represent the average observations from upward looking Eppley pyranometers at the 3- and 80-year sites. The above-canopy air temperature time series represents the average measurements collected at all three sites at heights reported in Table 1.

~1920, 1987, and 1999. These sites will be hereinafter referred to as the 80-, 15-, and 3-year sites. All three sites were within a 15-km radius of one another and were situated on flat terrain (Figure 1). The area around Delta Junction, Alaska, is composed of a combination of alluvial outwashes, floodplains, and low terraces dissected by glacial streams originating in the nearby Alaska Range [*Manies et al.*, 2004]. Although some areas in the Delta region are underlain by permafrost (typically those areas with north facing slopes or poorly drained soils), permafrost was not present within the fetch of our three, well-drained sites. Our sites were located near the Tanana River with elevations of 469 m above sea level (masl) for the 3-year site, 410 masl for the 15-year site, and 518 masl for the 80-year site. Because of their close proximity to one another these sites experienced similar climate and synoptic weather.

[12] Solar radiation, above-canopy air temperature, and 10-cm soil temperatures during our measurement period from 10 April 2002 through 9 April 2003 are shown in Figure 2. Average rainfall during the 2002 growing season was 12, 66, 45, 97, and 53 mm during May, June, July, August, and September, respectively, on the basis of the mean of two automated tipping bucket rain gauges installed at the 3- and 15-year sites.

2.1. The 3-Year Burn

[13] The Donnelly Flats fire occurred in June of 1999 just south of Delta Junction (63°55′N, 145°44′W) and burned ~7600 ha of black spruce (*Picea mariana*) [*Chambers and Chapin*, 2002]. The crown fire killed all of the aboveground vegetation and consumed much of the aboveground biomass and soil organic mat, so the mineral soil was an average of only 4 cm below the charred surface [*Manies et al.*, 2004]. Burning caused a reduction of approximately 7 ± 7 cm of the organic mat (profile and transect data that translated to about 1400 ± 600 g C m^{-2} [*Manies et al.*, 2004; J. C. Neff et al., Fire effects on soil organic matter content and composition in boreal soils, submitted to *Canadian Journal of Forest Research*, 2004]). The boles of the black spruce remained standing 3 years after the fire with a mean height of 4 m and a stand density of 2691 ± 778 dead trees per hectare (M. C. Mack, unpublished data, 2004). In 2002, ~30% of the surface was covered by bunch grasses (*Festuca altaica*) and deciduous shrubs (that had a height less than 1 m). The other 70% of the surface was not covered by vascular plants. Total aboveground biomass in 2002 (consisting of vegetation that had grown since the fire) was 105 ± 21 g biomass m^{-2} (M. C. Mack, The influence of fire on aboveground biomass and net primary productivity in boreal black spruce forests of interior Alaska, manuscript in preparation, 2005, hereinafter referred to as Mack, manuscript in preparation, 2005). A uniform fetch from the tower extended for more than 1 km in all directions. Moss cover expanded in each consecutive year since the burn and consisted of *Polytrichum* and *Ceratodon* species.

2.2. The 15-Year Burn

[14] The 15-year site was located southeast of Delta Junction (63°55′N, 145°23′W). The Granite Creek fire occurred in 1987 and burned ~2.0×10^4 ha [*Chambers and Chapin*, 2002]. The crown fire killed all of the aboveground vegetation, which consisted primarily of black spruce. The stem density of dead black spruce was 3200 ± 1329 ha^{-1} [*Chambers and Chapin*, 2002]. Many of the dead black spruce trees that were killed during the fire in 1987 remained standing in 2002, while others had fallen over. Many of the fallen trees were caught on the branches and boles of those remaining standing, creating in places a complex three-dimensional structure. In 2002, heterogeneous aspen and willow species dominated the overstory (*Populus tremuloides* and *Salix* spp.). Aspen had a mean canopy height of 5 m and a density of 3956 ± 370 tree ha^{-1} (M. C. Mack, unpublished data, 2004). Total aboveground biomass of aspen in 2001 (consisting of vegetation that had grown since the fire) was 1674 ± 436 g biomass m^{-2} (Mack, manuscript in preparation, 2005). The sparse understory vegetation included shrubs (*Salix* spp., *Ledum paustre*, *Rosa acicularis, Vaccinium uliginosum,* and *Vaccinium vitis-idaea*), black spruce (*Picea mariana*), and grasses (*Festuca* spp. and *Calamagrostis lapponica*), separated by patches of moss in open areas (*Polytrichum* spp.). The burn scar from the tower extended for more than 1 km to the south, west, and north and ~500 m to the east.

Table 1. Instrument Configuration and Heights at the Three Eddy Flux Sites

Instrument	Height,[a] m		
	3-Year Site	15-Year Site	80-Year Site
Sonic anemometer (CSAT3, Campbell Scientific, Inc.) and infrared gas analyzer (LiCor 7500, LI-COR, Inc.)	7.8	10.0	9.5
Net radiation (Q7.1, REBS, Inc.)	7.0	10.3	11.0
K↓/K↑ (precision spectral pyranometer, Eppley Laboratory, Inc.)	7.0	NA[b]	10.7
K↓ (LI 200 silicon pyranometer, LI-COR, Inc.)	9.0	11.4	11.4
Above-canopy photosynthetically active radiation (LI 190, LI-COR, Inc.)	9.0	11.4	11.4
Below-canopy photosynthetically active radiation (LI 190, LI-COR, Inc.)	0.1	0.2	NA[b]
Wind direction and wind speed (R. M. Young, Inc.)	9.0	12.0	11.8
Wind speed (R. M. Young, Inc.)	4.8	6.3	7.1
T/RH probe 1 (HMP45C, Vaisala, Inc.)	8.5	10.0	11.4
T/RH probe 2 (HMP45C, Vaisala, Inc.)	5.0	6.3	7.4
T/RH probe 3 (HMP45C, Vaisala, Inc.)	2.0	2.0	2.0
Atmospheric pressure (CS105 pressure sensor, Vaisala, Inc.)	1.0	2.0	1.7
Precipitation (TE525 MM rain gauge, Texas Electronics, Inc.)	1.0	1.0	NA[b]

[a]Reported heights are above ground level.
[b]NA indicates instruments unavailable.

2.3. The 80-Year Burn

[15] The 80-year site was located ~5 km to the south of the 3-year site (63°53′N, 145°44′W). The canopy overstory consisted of homogeneous stands of black spruce (*Picea mariana*) with a mean canopy height of 4 m and a mean age of 80 years based on tree ring measurements. In 2001, black spruce tree density was 3744 ± 462 tree ha^{-1}, and total aboveground biomass, consisting almost entirely of black spruce, was 2418 ± 186 g biomass m^{-2} (Mack, manuscript in preparation, 2005). The sparse understory consisted primarily of shrubs (*Ledum palustre*, *Vaccinium uliginosum*, and *V. vitis-idaea*). The dominant ground cover species were feathermoss (*Pleurozium schreberi* and *Rhytidium rugosum*) and lichen (*Cladonia* spp. and *Stereocaulon* spp.). Moss and soil organic layers had a mean depth of ~11 cm to mineral soil [*Manies et al.*, 2004]. The site extended from the tower for more than 1 km to the south, west, and north, with the shortest fetch to the east (~200 m).

3. Instruments and Methods

[16] Instrument heights varied at the three sites because of differences in vegetation height (Table 1). Turbulent fluxes of sensible heat (H), latent heat (LE), and carbon dioxide (CO_2) were measured at each site with an eddy covariance system that consisted of a three-dimensional sonic anemometer (CSAT3, Campbell Scientific, Inc.) and an open path carbon dioxide/water vapor (CO_2/H_2O) infrared gas analyzer (IRGA) (LI 7500, LI-COR, Inc.). The sonic anemometers measured fluctuations of the three components of wind velocity and fluctuations of sonic temperature of the atmosphere. IRGAs measured fluctuations of densities of water vapor and carbon dioxide. At each site the eddy covariance system was mounted at a height ~2 times that of the mean canopy (Table 1) on an aluminum tower (Climatronics Corp.).

[17] Sensor signals were recorded by data loggers (CR5000, Campbell Scientific, Inc.) at a rate of 10 Hz. Vertical fluxes of H and LE were obtained via 30-min mean covariance between vertical velocity (w') and the respective scalar (c') fluctuation. Turbulent fluctuations were calculated as the difference between the instantaneous and the 30-min mean quantities. We made corrections to account for density effects on latent heat flux caused by heat and water transfer following *Webb et al.* [1980]. Because the temperature obtained from the sonic anemometer is the sonic temperature and because the crosswind effect should be taken into account [*Kaimal and Finnigan*, 1994], we applied a correction following that established by *Liu et al.* [2001]. We checked the original 10-Hz time series of temperature, H_2O, and CO_2 for spiking/noise. Data points were replaced through linear interpolation when their magnitudes exceeded 5σ of the half hour mean (where σ denotes standard deviation). Some flux data were rejected when winds were blowing through the towers and when the data did not pass a quality check [*Foken and Wichura*, 1996]. In addition, in our analysis and site comparisons we only included flux data from each site during periods when all three sites were simultaneously active. We report the number of data points that met these criteria for each season in Table 2.

[18] Along with the turbulent fluxes a variety of micrometeorological variables were also measured as 30-min averages of 1-s readings at our three sites (see Table 1). Net radiation (Rn) was measured with net radiometers (Q-7.1, Radiation and Energy Balance Systems (REBS), Inc.) at all three sites. Incoming and reflected global solar radiation was measured with precision spectral pyranometers (Eppley Laboratory, Inc.) at the 3- and 80-year sites. Air temperature and relative humidity were measured at three heights at all three sites with temperature/humidity probes (HMP45C, Vaisala, Inc.). A wind sentry unit (model 03001, R. M. Young, Inc.) was mounted at the top of the tower to measure wind speed and wind direction, while another wind speed sensor (model 03101, R. M. Young, Inc.) was mounted on each tower at an intermediate height.

[19] At three sites within 2–4 m of the tower base we measured soil temperature profiles. In each profile, thermocouples were placed at 0-, 2.5-, 5-, 10-, and 20-cm depths below the surface. In two of the three profiles at each site we also measured the soil heat flux (G_{10}) at a depth of 10 cm using soil heat flux plates (model HFT3, REBS, Inc.). The soil heat flux (G_0) at the surface was estimated using the thermal conductivity equation. The method for calculating soil thermal conductivity was obtained from National Center for Atmospheric Research Community Land Model

Table 2. Seasonal Energy Balance Closure at the Three Sites

		3-Year Site			15-Year Site			80-Year Site		
Season	N[a]	Slope	Intercept	r^2	Slope	Intercept	r^2	Slope	Intercept	r^2
Spring	3839	0.70	8.3	0.87	0.77	6.1	0.88	0.81	8.5	0.93
Summer	3241	0.80	9.0	0.83	0.83	7.0	0.83	0.86	10.5	0.88
Autumn	3413	0.73	−2.2	0.85	0.77	−2.5	0.80	0.76	4.4	0.84
Winter	1150	0.75	−5.2	0.80	0.78	1.7	0.80	0.72	−1.7	0.79

[a] N represents the number of half-hourly data within each season when all three eddy covariance flux systems were simultaneously operational. Only data collected during these periods were used for comparisons shown in this paper. Linear regression coefficients were obtained from plots of half-hourly data of H + LE (W m^{-2}) versus Rn − G_0 (W m^{-2}).

2.0 model, which is based on the work by *Farouki* [1981]. Using this approach, we also estimated soil heat fluxes at 10 cm on the basis of a vertical profile of soil temperatures at 10 and 20 cm and then validated these soil heat flux estimates for the summer period (June, July, and August) using data from the soil heat flux plates (G_{10}). Precipitation totals were measured at half-hourly intervals at both the 15- and the 3-year sites with an automated tipping bucket rain gauge (model TE525, Campbell Scientific, Inc.).

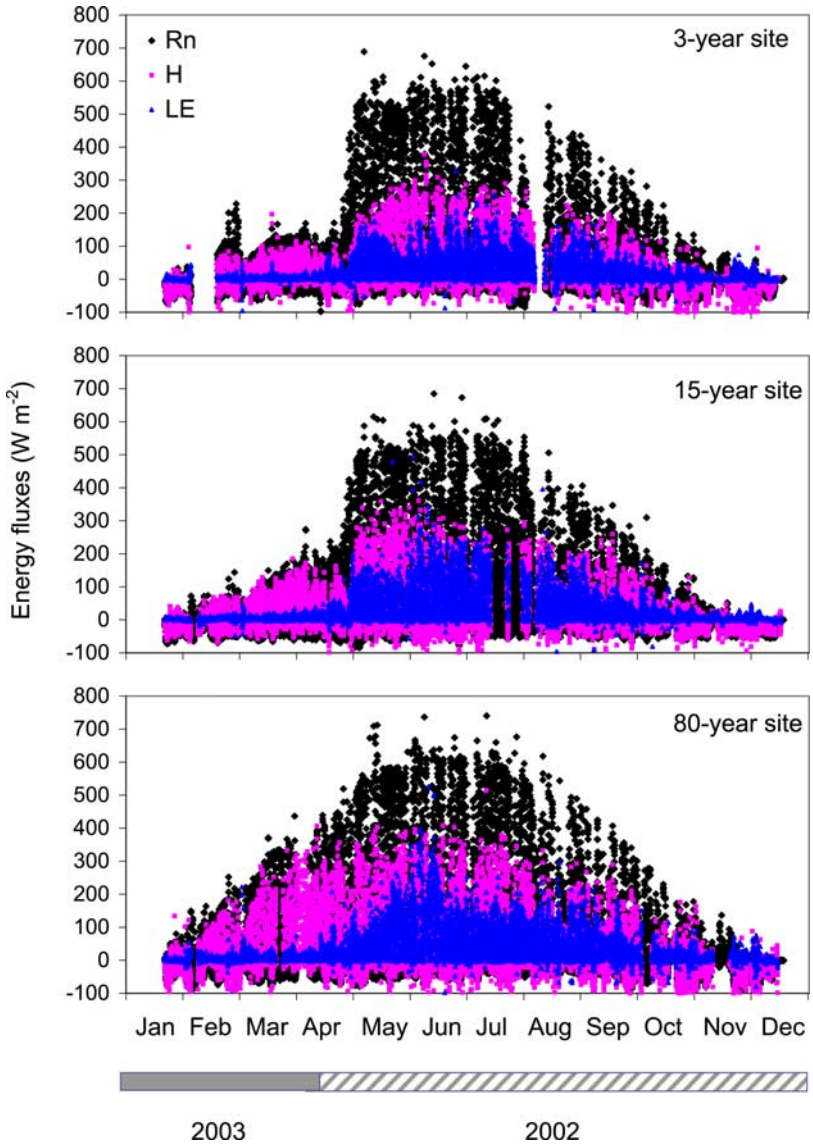

Figure 3. Half-hourly net radiation, sensible heat flux, and latent heat flux measured at the three sites from 10 April 2002 to 9 April 2003. Some data gaps were caused by power interruptions and instrument failure and repair. Loss of snow cover occurred rapidly at the 3- and 15-year sites during the last week of April.

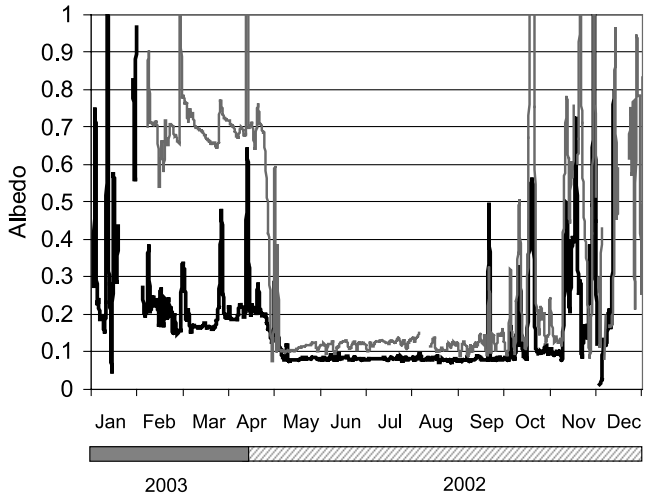

Figure 4. Seasonal course of averaged midday albedo measured at both the 3-year site (shaded line) and the 80-year site (solid line). During fall, winter, and spring, large variations in midday albedo were caused by snowstorms.

[20] Closure of the energy balance is commonly accepted as an important factor in assessing eddy covariance data. Usually, linear regression coefficients (slope and intercept) from an ordinary least squares fit of $H + \mathrm{LE}$ versus $\mathrm{Rn} - G_0$ are used to evaluate the energy closure. However, because the data were subject to measurement errors not only in the turbulent fluxes but also in the available energy, we used a linear regression that accounted for errors in both coordinates [*Press et al.*, 1992]. Using this method and all the 30-min data for the three sites within a seasonal period, the slopes and intercepts of $H + \mathrm{LE}$ versus $\mathrm{Rn} - G_0$ are shown in Table 2. In general, the slopes were less than 1 for the three sites, ranging from 0.70 to 0.80 for the 3-year site, from 0.77 to 0.83 for the 15-year site, and from 0.72 to 0.86 for the 80-year site. Closure appeared to be higher during summer than during the other seasons. In spring we did not attempt to estimate the energy required to melt snow and to thaw soils (the heat of fusion), and this may be partially responsible for the lower closure. Although a surface energy imbalance is common in current flux measurements using the eddy covariance technique, the causes for this imbalance remain unclear [*Wilson et al.*, 2002].

4. Results

4.1. Annual Overview

[21] Half-hourly measurements of net radiation, sensible heat, and latent heat over the course of a year are presented in Figure 3. A primary impact of fire was to decrease annual net radiation, primarily as a result of increased snow cover in postfire ecosystems during spring and subsequent decreases in the amount of shortwave radiation absorbed by the surface (Figures 3 and 4). Averaged over the year, net radiation was 31% lower at both the 3- and the 15-year sites as compared with the 80-year site (Table 3). At the 3-year site, 59% of the annual decrease in net radiation occurred during spring, with the remainder occurring during summer (21%), winter (18%), and fall (2%). At the 15-year site, 53% of the annual decrease in net radiation occurred during spring, with the remainder occurring during summer (32%) and winter (15%).

[22] Fire also substantially altered turbulent energy fluxes. Annual sensible heat fluxes were reduced by 55% at the 3-year site and by 52% at the 15-year site. At the 3-year site this sensible heat reduction occurred primarily during the spring (76%), with the remainder occurring during summer (14%), fall (−2%), and winter (12%). At the 15-year site the reduction in the annual sensible heat flux occurred mostly during spring (58%) and summer (36%), with smaller changes during fall (−8%) and winter (14%). At both of the recently disturbed sites, sensible heat fluxes were greater than at the 80-year site during fall (making a small negative contribution to the total annual reduction).

[23] Annual ET also decreased immediately following fire by 33% for the 3-year site as compared with the 80-year site (Table 3). Although the 15-year site had the highest ET during summer (Table 3) and particularly during a drought in early July (Figure 5), this site had consistently lower ET during spring and fall (before leaf emergence and after leaf senescence) as compared with the 80-year site. The lower ET rates at the margins of the growing season at the 15-year site (during periods when the deciduous aspen and willow canopy was leafless) contributed to an annual ET flux (283 mm yr^{-1}) that was, within measurement error, the same as that observed at the 80-year site (301 mm yr^{-1}).

[24] Because fire consumed much of the overstory and understory vegetation and because there was only modest regrowth in the 3-year interval since the fire, the 3-year site had the largest seasonal range of soil temperatures (Figure 2) and ground heat fluxes (Figure 5). Compared with the

Table 3. Seasonally Averaged Radiation Budget and Energy Fluxes

Site	$K_\downarrow$	Rn	G_0	$\mathrm{Rn} - G_0$	H	LE	Bo
Spring (March, April, and May)[a]							
3-year	165.2	57.8	4.5	53.3	21.0	14.9	2.2
15-year	165.2	61.2	5.0	56.2	31.1	18.0	2.5
80-year	165.2	98.0	2.5	95.5	56.8	23.3	3.5
Summer (June, July, and August)							
3-year	189.8	124.0	12.1	111.9	44.3	36.2	1.6
15-year	189.8	116.6	11.0	105.6	35.1	59.0	0.9
80-year	189.8	138.3	9.4	128.9	50.7	54.8	1.3
Autumn (September, October, and November)							
3-year	40.3	1.8	−2.5	4.3	−9.0	9.8	1.4
15-year	40.3	3.2	−3.0	6.2	−6.2	9.7	1.0
80-year	40.3	2.9	−1.0	3.9	−9.9	13.6	1.2
Winter (December, January, and February)							
3-year	14.0	−31.1	−10.1	−21.0	−18.7	3.3	0.5
15-year	14.0	−29.0	−9.3	−19.7	−19.3	3.1	−0.5
80-year	14.0	−18.7	−7.0	−11.7	−13.1	3.7	2.4
All Year (January–December)							
3-year	102.3	38.1	1.0	37.1	9.4	16.1	1.9
15-year	102.3	38.0	0.9	37.1	10.1	22.5	2.0
80-year	102.3	55.1	1.0	54.2	21.1	23.9	1.7

[a]These measurements represent the net totals averaged over each day and over all of the days within a season when measurements were simultaneously available at all three sites. $K_\downarrow$ is solar radiation (W m^{-2}) averaged from the 3-year site and the 80-year site; Rn is net radiation (W m^{-2}); G_0 is ground heat flux at 0 cm (W m^{-2}); H is sensible heat flux (W m^{-2}); LE is latent heat flux (W m^{-2}); and Bo is averaged midday Bowen ratio, the ratio of the sensible heat flux to the latent heat flux.

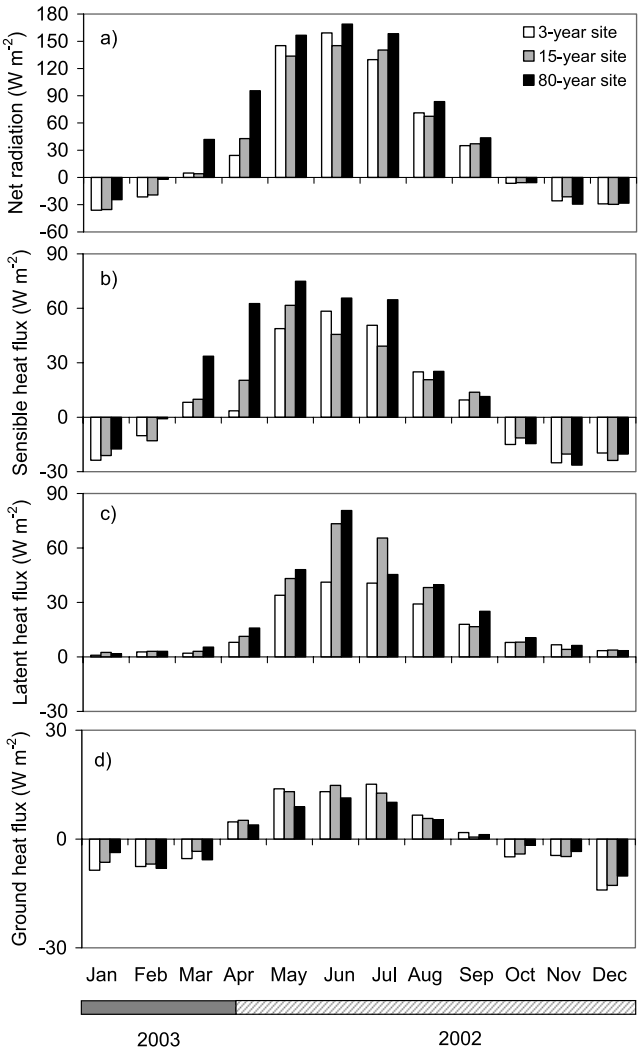

Figure 5. Monthly averaged (a) net radiation, (b) sensible heat flux, (c) latent heat flux, and (d) ground heat flux for the three sites. Figures 5, 6, and 8 were constructed only from periods when all three eddy covariance systems were simultaneously active.

recently disturbed sites, soil temperatures and ground heat fluxes at the 80-year site were damped during both summer and winter (Figure 5).

4.2. Seasonal Dynamics

4.2.1. Spring

[25] Loss of snow cover occurred rapidly in the two postfire ecosystems and had substantial impacts on net radiation (Figure 3). Complete loss of snow cover occurred at the 3-year site in less than a week starting around 26 April and was accompanied by a change in midday albedo from 0.7 to 0.1 (Figure 4). Over this same time interval, net radiation increased by a factor of 5 at the 3-year site and by a factor of 3 at the 15-year site (Figure 3). In contrast, net radiation increased more gradually at the 80-year black spruce forest, parallel with increases in solar radiation.

[26] A second important step change during spring occurred with the emergence of leaves on the aspen trees at the 15-year site. During the 3 weeks prior to leaf emergence (that occurred during the week of 23 May), net radiation was partitioned primarily into sensible heat fluxes (with a midday Bowen ratio of 1.9), whereas in the 3 weeks after leaf emergence, latent heat fluxes increased by over 50%, and the midday Bowen ratio decreased to 1.2 (Figure 3).

[27] During spring, much of the decrease in net radiation at the 3-year site as compared with the 80-year site can be attributed to a higher albedo. By assuming that downward longwave radiation was the same at the two sites (since they had very similar diurnal and seasonal patterns of incoming shortwave radiation and thus cloud cover) we estimated perturbations to net radiation from changes in net shortwave radiation and surface emission of longwave radiation. On the basis of mean values of solar radiation and albedo for spring (Table 4) the decrease in the net shortwave radiation flux (caused by the increase in albedo at the 3-year site) reduced net radiation by $\sim$40 W m^{-2} as compared with the 80-year site. Increased surface temperature (and thus greater surface emission of longwave radiation) at the 3-year site reduced net radiation by an additional 4.5 W m^{-2}. The sum of contributions from these two processes ($-$44 W m^{-2}) compares reasonably well with that measured directly using our net radiometers ($-$41 W m^{-2}) (Table 3).

[28] The decreased net radiation and slightly increased ground heat fluxes at the disturbed sites caused a reduction in the available energy flux (Rn $-$ G_0) by 44% (42 W m^{-2}) at the 3-year site and by 41% (39 W m^{-2}) at the 15-year site. Concurrently, there was a substantial reduction in both sensible and latent heat fluxes at the two recently disturbed sites (Figure 6). At the 3-year site, sensible heat flux was reduced by 63% (36 W m^{-2}), while latent heat flux was reduced by 36% (8 W m^{-2}). Similarly, at the 15-year site, sensible heat flux was reduced by 45% (26 W m^{-2}), while latent heat flux was reduced by 23% (5 W m^{-2}).

4.2.2. Summer

[29] During summer, midday albedo was consistently higher at the 3-year site (0.12) than at the 80-year site (0.08), even though the absolute difference in albedo between the two sites was small. No albedo measurements were made at the 15-year site, but previous measurements at this site in 1999 showed that the midday albedo was 0.13 [*Chambers and Chapin*, 2002]. According to satellite data

Table 4. Influence of Albedo and Soil Surface Temperature on Net Radiation[a]

	Spring	Summer
$K_\downarrow$	165, W m^{-2}	190, W m^{-2}
$\Delta\alpha$	0.24	0.04
ΔT	0.99	6.9
ΔSW	$-$40	$-$7.7
ΔLW	$-$4.5	$-$30.5
ΔRn	$-$44.5	$-$38.2

[a] $K_\downarrow$ represents downward solar radiation (W m^{-2}); $\Delta\alpha$, ΔT, and ΔSW represent measured differences between the 3-year site and the 80-year site for albedo, soil surface temperature (K), and shortwave radiation (W m^{-2}). ΔLW represents the difference in longwave radiation (W m^{-2}) between the two sites that was estimated using the measured soil surface temperatures to estimate surface emission of longwave radiation and by assuming the downward longwave radiation flux at the two sites was the same because of their close proximity to one another. ΔRn represents the net radiation difference between the two sites (W m^{-2}) as estimated from the sum of the shortwave and longwave components given in Table 4.

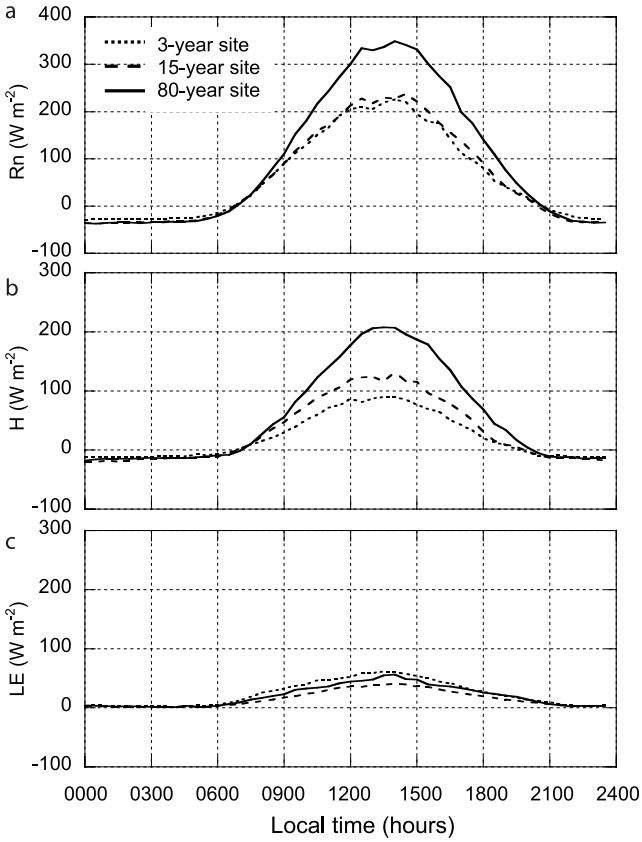

Figure 6. Average diurnal cycles of (a) net radiation, (b) sensible heat flux, and (c) latent heat flux during spring (March, April, and May).

from Moderate Resolution Imaging Spectroradiometer, all three sites had maximum values of leaf area index (LAI) during July (Figure 7). The 15-year site, with an abundance of deciduous aspen and willow, showed the greatest increase in LAI between May and July (Figure 7).

[30] Although the difference was not as great as that observed during spring, net radiation during summer was lower in the recently disturbed sites than at the 80-year site (Figure 8). From an analysis of the radiation budget the decrease in summer net radiation at the 3-year site appears to be driven more by an increase in surface temperature (and thus an increase in surface emission of longwave radiation) than by the higher albedo values observed at this site (Table 4). From previous observations it is likely that the relatively high albedo at the 15-year site contributed, in part, to the reduction in net radiation that we observed at this site during summer (Figure 8) [*Chambers and Chapin*, 2002].

[31] Sensible heat fluxes were reduced at both the 3-year (13%, 6 W m^{-2}) and 15-year sites (31%, 16 W m^{-2}) during summer, as compared with the 80-year site. These reductions were smaller than those observed during spring but were consistent in magnitude with measurements from previous reports [*Chambers and Chapin*, 2002]. The reduced sensible heat flux at the 15-year site was caused at least partially by the high leaf area and canopy conductance of the deciduous overstory that led to high ET fluxes and low midday Bowen ratios. Even during a period of drought in July the 15-year site maintained high ET fluxes, in contrast with the 80-year site where a much greater fraction

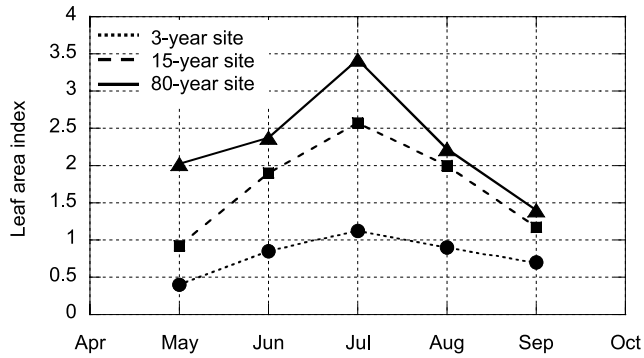

Figure 7. Monthly variation of leaf area index (LAI) during the 2002 growing season derived from Moderate Resolution Imaging Spectroradiometer (MODIS) satellite data for the 3-year site (circles), the 15-year site (squares), and the 80-year site (triangles). The values presented here are the average of four 250-m pixels within the footprint of each tower. The data are from the MODIS version 4 LAI product developed by *Myneni et al.* [2002]. The LAI estimated from the satellite represents the leaf area of the site projected vertically on a horizontal plane and has units of m^2 m^{-2}.

of the available energy during this time was dissipated in the form of sensible heat (Figures 3 and 5).

4.2.3. Fall

[32] During fall, net radiation, ground heat fluxes, and available energy were similar at all three sites (Table 3 and

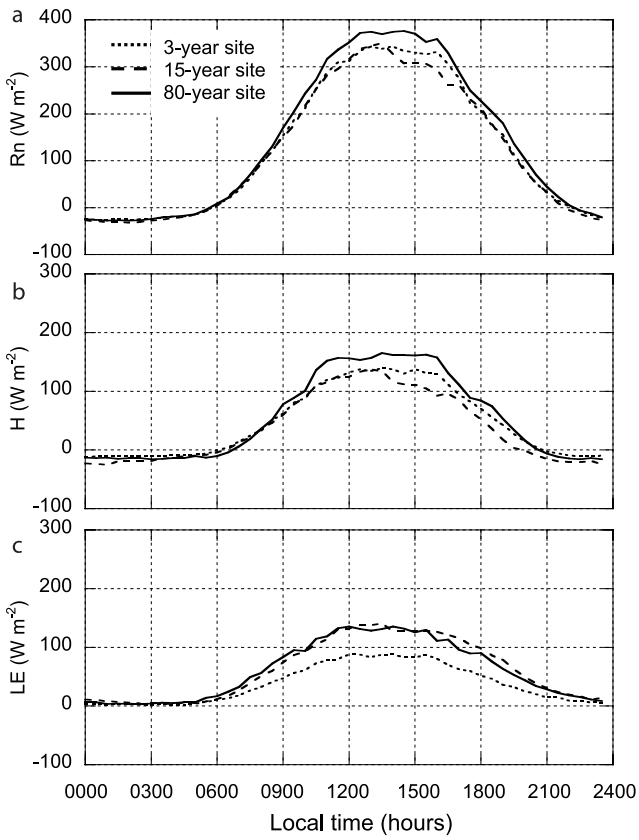

Figure 8. Average diurnal cycles of (a) net radiation, (b) sensible heat flux, and (c) latent heat flux during summer (June, July, and August).

Figure 5). Transfer of heat to the atmosphere by latent heat was almost perfectly balanced by warming of the surface via sensible heat exchange. During this transition period many of the snow events quickly melted, particularly during September and October (Figure 4), and so large differences in albedo between the sites were not sustained. Overall, latent heat flux was higher at the 80-year site than at the recently disturbed sites by $\sim$4 W m^{-2}, possibly as a result of the extended conifer growing season in September (Figure 5) and the more efficient capture and evaporation of precipitation events by the spruce canopy and moss layer at the 80-year site (see section 5 for more detail).

4.2.4. Winter

[33] During winter, total solar radiation was low, limiting the total impact of differences in plant functional types on the annual surface energy budget. However, differences in albedo between the sites (caused by differences in snow cover and the vegetation cover) were now persistent and contributed to greater absorption of solar radiation by the 80-year site. Both the lower albedo and a reduced loss of soil heat at the 80-year site contributed to higher values of net radiation fluxes than at the two recently disturbed sites.

5. Discussion

5.1. Vegetation-Climate Feedbacks

[34] Our study provides evidence that large disturbances within the boreal forest caused by fire will increase albedo and will decrease sensible heat fluxes, as compared with what might be inferred in climate models that represent the boreal forest with a mature, unburned conifer vegetation type. The large decreases in annual sensible heat observed here in postfire ecosystems support the idea proposed by *Eugster et al.* [2000] that changes in stand age within the boreal biome can have comparable impacts on the atmosphere as shifts in the spatial extent of boreal and tundra biomes. In this context an important question that emerges is the degree to which the northward movement of the boreal forest tree line is coupled to an increase in the disturbance regime within the boreal forest interior. With warming both processes are likely to occur [*Flannigan and Van Wagner*, 1991; *Foley et al.*, 1994; *Kasischke et al.*, 1995; *Kasischke and Stocks*, 2000] and may potentially cancel each other with respect to their impact on climate. A related question concerns the southern border of the boreal zone: Will it remain static or migrate northward with climate warming? An expansion of grasslands and deciduous forest species in southern boreal regions would be expected to reduce net radiation and sensible heat fluxes by mechanisms similar to those documented here. Movement of the southern border of the boreal forest has the potential to have an even larger impact on Northern Hemisphere climate than the movement of the northern tree line because of the higher levels of incoming solar radiation at lower latitudes. The tree mortality–associated changes in vegetation at the southern boundary may also occur more rapidly than tree invasion at the northern tree line.

[35] Although we currently do not know the relative importance of these feedbacks at continental and panboreal scales, components required for this calculation are becoming available. Energy budget information from a wide variety of northern ecosystems (in various stages of succession) is now being compiled and archived as a part of FLUXNET [*Baldocchi et al.*, 2001]. Linking this information with observed distributions of stand age and species composition will enable us in the future to estimate the sensitivity of regional energy exchange to shifts in the disturbance regime. In addition to stand age, burn severity is another key variable linked with the disturbance regime that will be critical for this analysis. An increase in the ratio of crown fires to ground fires in Siberia, for example, could lead to climate cooling via the increases in spring snow cover and albedo described here, even if the fire return time remained the same.

[36] In addition to fire, stand-replacing insect outbreaks significantly affect the age distribution and carbon balance of boreal forests [*Kurz and Apps*, 1995] and may change with global warming [*Volney and Fleming*, 2000]. Insect outbreaks probably lead to similar trajectories of postdisturbance changes in the annual surface energy budget to those reported here for fire. We hypothesize, however, that decreases in atmospheric heating in the decades following a stand-replacing insect outbreak are smaller than those following fire because the forest canopy typically remains more intact for the case of an insect outbreak. A more intact canopy of dead trees would reduce the exposure of the snowpack during spring and would increase surface roughness and net radiation throughout the year. As far as we know, no year-round eddy covariance measurements of the surface energy budget have been reported following a stand-replacing insect outbreak, although summer CO_2 fluxes have been reported from a boreal chronosequence where one of the stands may have been established following such an event [*Roser et al.*, 2002].

5.2. Impacts of Fire on Annual Evapotranspiration

[37] Measurements from this study and previous reports clearly show that during summer, deciduous forests have higher ET (and thus lower Bowen ratios) than nearby coniferous forests [*Baldocchi et al.*, 2000; *Eugster et al.*, 2000]. Our measurements at the 15- and 80-year sites suggest that this pattern is nonexistent or even reversed when ET is integrated over a year. Several different mechanisms probably contribute to this result.

[38] During spring and fall, albedo in the black spruce ecosystems is low, thus increasing net radiation and available energy to drive both latent and sensible heat fluxes. In parallel, observations from our sites (data not shown) and other studies [e.g., *Schulze and Fuchs*, 1997; *Falge et al.*, 2002] show that periods of photosynthesis and transpiration are extended in conifer ecosystems during both spring and fall as compared with nearby deciduous forest ecosystems. Thus, even though ET is lower in black spruce than in the aspen in midsummer, the extended black spruce growing season may lead to a comparable annual flux.

[39] In addition, the moss layer and well-developed organic horizons in black spruce ecosystems may act as a buffer for soil moisture, absorbing high-intensity rain events and limiting runoff and drainage below the rooting zone. This would increase the total pool of water available for annual ET, even if absorption and evaporation of summer rain by the moss layer limited water availability to black spruce. The role of the moss and organic soil layers may be

particularly important during the spring thaw, when rain or periods of warm temperatures trigger snowmelt.

[40] Further, during winter and spring it is likely that the conifer overstory contributes in several different ways to increased precipitation storage. Specifically, the complex three-dimensional structure of the conifer overstory may enhance snow deposition and accumulation at the base of the trees in windy environments in contrast with the more direct coupling of the snow surface to the atmosphere that would be expected in postfire ecosystems [e.g., *Sturm et al.*, 2001]. For example, mean snow depth measured by ultrasonic distance sensors (model SR50, Campbell Scientific, Inc.) from 1 February to 20 April of 2002 was 20 cm for the 3-year site and 45 cm for the 80-year site. Also, shading of the snow surface by the black spruce overstory during spring creates a patchy pattern of snow cover and prolongs the duration of the thaw. At our sites, loss of snow cover during spring occurred more rapidly in the two ecosystems recently disturbed by fire (shown indirectly by the rapid increases in net radiation at the 3- and 15-year sites in Figure 3 and the rapid decrease in albedo at the 3-year site in Figure 4). Because of the sudden loss of snow cover at the 3- and 15-year sites (and because the underlying soils remained frozen) it is likely that runoff was enhanced at these sites.

5.3. Uncertainties

[41] Our study of the surface energy budget is one of the first to provide observations made over a full year from boreal forest ecosystems. Given the uncertainties introduced from the experimental (and instrumental) approaches used here, along with the limited time period of the analysis (1 year), the limited number of sites in the fire chronosequence, and the diversity of postfire ecosystem trajectories, caution needs to be taken in extrapolating these results to larger spatial scales. A key finding from our analysis was that even though incoming solar radiation was lower in spring than in summer (Table 3), the large difference in albedo between the recently disturbed sites and the 80-year site (Figure 4) during spring resulted in the largest absolute site differences in net radiation and sensible heat of any seasonal period. The differences in the surface energy budget observed here between sites are probably most robust during spring and summer, when solar radiation, net radiation, sensible heat, and latent heat fluxes are large and yield a high signal-to-noise ratio that can be detected by micrometeorological and eddy covariance instruments. In contrast, relatively low energy inputs during fall and winter make it more challenging to separate site-to-site differences in the surface energy budget from small but persistent offsets caused, for example, by biases introduced during instrument calibration and differences in energy balance closure among our sites.

6. Conclusions

[42] Examining the energy budget over a full year, we found that in postfire ecosystems, net radiation was reduced by ~30% and that sensible heat fluxes were reduced by ~50%. The largest difference between prefire and postfire sites occurred during spring, emphasizing the need for more energy budget measurements during periods outside of the growing season. These observations strengthen the hypothesis, derived mostly from summer observations, that increased fire frequency could lead to regional cooling in high-latitude regions via an expansion of areas dominated by deciduous vegetation cover. This work provides a direct means to test and to validate global climate models attempting to capture vegetation-climate feedbacks in northern terrestrial regions.

[43] **Acknowledgments.** We thank M. Mack, E. A. G. Schuur, K. Treseder, and J. Harden for providing data on vegetation and soils at these sites and S. D. Chambers for providing invaluable insight about eddy covariance measurement techniques in boreal ecosystems. C. Dunn, J. Henkelman, and J. Smith contributed substantially to the development of these sites. J. Garron provided invaluable technical assistance throughout the year of this study. We are grateful for constructive suggestions and comments from three anonymous reviewers. This work was supported by an NSF RAISE grant OPP-0097439, the Powell Foundation, and a gift from the Davidows to Caltech.

References

Amiro, B. D. (2001), Paired-tower measurements of carbon and energy fluxes following disturbance in the boreal forest, *Global Change Biol.*, *7*(3), 253–268.

Amiro, B. D., J. I. MacPherson, and R. L. Desjardins (1999), BOREAS flight measurements of forest-fire effects on carbon dioxide and energy fluxes, *Agric. For. Meteorol.*, *96*(4), 199–208.

Baldocchi, D., F. M. Kelliher, T. A. Black, and P. G. Jarvis (2000), Climate and vegetation controls on boreal zone energy exchange, *Global Change Biol.*, *6*(S1), 69–83.

Baldocchi, D., et al. (2001), FLUXNET: A new tool to study the temporal and spatial variability of ecosystem-scale carbon dioxide, water vapor and energy flux densities, *Bull. Am. Meteorol. Soc.*, *82*, 2415–2434.

Betts, A. K., and J. H. Ball (1997), Albedo over the boreal forest, *J. Geophys. Res.*, *102*(D24), 28,901–28,909.

Blanken, P. D., T. A. Black, H. H. Neumann, G. den Hartog, P. C. Yang, Z. Nesic, and X. Lee (2001), The seasonal water and energy exchange above and within a boreal aspen forest, *J. Hydrol.*, *245*, 118–136.

Bonan, G. B., D. Pollard, and S. L. Thompson (1992), Effects of boreal forest vegetation on global climate, *Nature*, *359*, 716–718.

Bonan, G. B., F. S. Chapin III, and S. L. Thompson (1995), Boreal forest and tundra ecosystems as components of the climate system, *Clim. Change*, *29*(2), 145–167.

Chambers, S. D., and F. S. Chapin III (2002), Fire effects on surface-atmosphere energy exchange in Alaskan black spruce ecosystems: Implications for feedbacks to regional climate, *J. Geophys. Res.*, *107*(D1), 8145, doi:10.1029/2001JD000530.

Chambers, S. D., J. Beringer, J. T. Randerson, and F. S. Chapin III (2005), Fire effects on net radiation and energy partitioning: Contrasting responses of tundra and boreal forest ecosystems, *J. Geophys. Res.*, *110*, D09106, doi:10.1029/2004JD005299.

Chapin, F. S., III, et al. (2000), Arctic and boreal ecosystems of western North America as components of the climate system, *Global Change Biol.*, *6*(S1), 211–223.

Conard, S. G., A. I. Sukhinin, B. J. Stocks, D. R. Cahoon, E. P. Davidenko, and G. A. Ivanova (2002), Determining effects of area burned and fire severity on carbon cycling and emissions in Siberia, *Clim. Change*, *55*(1–2), 197–211.

Eaton, A. K., W. R. Rouse, P. M. Lafleur, P. Marsh, and P. D. Blanken (2001), Surface energy balance of the western and central Canadian subarctic: Variations in the energy balance among five major terrain types, *J. Clim.*, *14*(17), 3692–3703.

Eugster, W., et al. (2000), Northern ecosystems and land-atmosphere energy exchange in Arctic tundra and boreal forest: Available data and feedbacks to climate, *Global Change Biol.*, *6*(S1), 84–115.

Falge, E., et al. (2002), Seasonality of ecosystem respiration and gross primary production as derived from FLUXNET measurements, *Agric. For. Meteorol.*, *113*(1–4), 53–74.

Farouki, O. T. (1981), *Thermal Properties of Soils*, *CRREL Monogr. 81-1*, Cold Reg. Res. and Eng. Lab., Hanover, N. H.

Flannigan, M. D., and C. E. Van Wagner (1991), Climate change and wildfire in Canada, *Can. J. For. Res.*, *21*(1), 66–72.

Foken, T., and B. Wichura (1996), Tools for quality assessment of surface-based flux measurements, *Agric. For. Meteorol.*, *78*(1–2), 83–105.

Foley, J. A., J. E. Kutzbach, M. T. Coe, and S. Levis (1994), Feedbacks between climate and boreal forests during the Holocene epoch, *Nature*, *371*, 52–54.

French, N. H. F. (2002), The impact of fire disturbance on carbon and energy exchange in the Alaskan boreal region: A geospatial analysis, Ph.D. thesis, 105 pp., Univ. of Mich., Ann Arbor.

Gallimore, R. G., and J. E. Kutzbach (1996), Role of orbitally-induced changes in tundra area in the onset of glaciation, *Nature*, *381*, 503–505.

Girardin, M. P., J. Tardif, M. D. Flannigan, B. M. Wotton, and Y. Bergeron (2004), Trends and periodicities in the Canadian drought code and their relationships with atmospheric circulation for the southern Canadian boreal forest, *Can. J. For. Res.*, *34*(1), 103–119.

Hansen, J., and L. Nazarenko (2004), Soot climate forcing via snow and ice albedos, *Proc. Natl. Acad. Sci. U. S. A.*, *101*, 423–428.

Harding, R. J., and J. W. Pomeroy (1996), The energy balance of the winter boreal landscape, *J. Clim.*, *9*(11), 2778–2787.

Kaimal, J. C., and J. J. Finnigan (1994), *Atmospheric Boundary Layer Flows: Their Structure and Measurement*, 289 pp., Oxford Univ. Press, New York.

Kasischke, E. S., and B. J. Stocks (Eds.) (2000), *Fire, Climate Change, and Carbon Cycling in the Boreal Forest*, 461 pp., Springer, New York.

Kasischke, E. S., N. L. Christensen Jr., and B. J. Stocks (1995), Fire, global warming, and the carbon balance of boreal forests, *Ecol. Appl.*, *5*(2), 437–451.

Kurz, W. A., and M. J. Apps (1995), An analysis of future carbon budgets of Canadian boreal forests, *Water Air Soil Pollut.*, *82*(1–2), 321–331.

Liston, G. E., J. P. McFadden, M. Sturm, and R. A. Pielke (2002), Modelled changes in Arctic tundra snow, energy and moisture fluxes due to increased shrubs, *Global Change Biol.*, *8*(1), 17–32.

Liu, H. P., G. Peters, and T. Foken (2001), New equations for omnidirectional sonic temperature variance and buoyancy heat flux with a sonic anemometer, *Boundary Layer Meteorol.*, *100*, 459–468.

Manies, K. L., J. W. Harden, S. R. Silva, P. H. Briggs, and B. M. Schmid (2004), Soil data from *Picea mariana* stands near Delta Junction, Alaska of different ages and soil drainage type, *U.S. Geol. Surv. Open File Rep., 2004-1271*.

Michalek, J. L., N. H. F. French, E. S. Kasischke, R. D. Johnson, and J. E. Colwell (2000), Using Landsat TM data to estimate carbon release from burned biomass in an Alaskan spruce forest complex, *Int. J. Remote Sens.*, *21*(2), 323–338.

Myneni, R. B., et al. (2002), Global products of vegetation leaf area and fraction absorbed PAR from year one of MODIS data, *Remote Sens. Environ.*, *83*, 214–231.

Ohta, T., K. Suzuki, Y. Kodama, J. Kubota, Y. Kominami, and Y. Nakai (1999), Characteristics of the heat balance above the canopies of evergreen and deciduous forests during the snowy season, *Hydrol. Processes*, *13*(14–15), 2383–2394.

O'Neill, K. P., E. S. Kasischke, and D. D. Richter (2003), Seasonal and decadal patterns of soil carbon uptake and emission along an age sequence of burned black spruce stands in interior Alaska, *J. Geophys. Res.*, *108*(D1), 8155, doi:10.1029/2001JD000443.

Press, W. H., B. P. Flannery, S. A. Teukolsky, and W. T. Vetterling (1992), *Numerical Recipes in FORTRAN 77: The Art of Scientific Computing*, 2nd ed., 963 pp., Cambridge Univ. Press, New York.

Roser, C., L. Montagnani, E. D. Schulze, D. Mollicone, O. Kolle, M. Meroni, D. Papale, L. B. Marchesini, S. Federici, and R. Valentini (2002), Net CO_2 exchange rates in three different successional stages of the "dark taiga" of central Siberia, *Tellus, Ser. B*, *54*(5), 642–654.

Schulze, E.-D., and M. I. Fuchs (1997), Spatial distribution of photosynthetic capacity and performance in a mountain spruce forest of northern Germany, III: The significance of the evergreen habit, *Oecologia*, *30*, 239–248.

Serreze, M. C., J. E. Walsh, F. S. Chapin III, T. Osterkamp, M. Dyurgerov, V. Romanovsky, W. C. Oechel, J. Morison, T. Zhang, and R. G. Barry (2000), Observational evidence of recent change in the northern high-latitude environment, *Clim. Change*, *46*(1–2), 159–207.

Skinner, W. R., M. D. Flannigan, B. J. Stocks, D. L. Martell, B. M. Wotton, J. B. Todd, J. A. Mason, K. A. Logan, and E. M. Bosch (2002), A 500 hPa synoptic wildland fire climatology for large Canadian forest fires, 1959–1996, *Theor. Appl. Climatol.*, *71*(3–4), 157–169.

Stocks, B. J., et al. (2002), Large forest fires in Canada, 1959–1997, *J. Geophys. Res.*, *107*(D1), 8149, doi:10.1029/2001JD000484.

Sturm, M., J. P. McFadden, G. E. Liston, F. S. Chapin III, C. H. Racine, and J. Holmgren (2001), Snow-shrub interactions in Arctic tundra: A hypothesis with climatic implications, *J. Clim.*, *14*(3), 336–344.

Thomas, G., and P. R. Rowntree (1992), The boreal forests and climate, *Q. J. R. Meteorol. Soc.*, *118*(505), 469–497.

Treseder, K. K., M. C. Mack, and A. Cross (2004), Relationships among fires, fungi, and soil dynamics in Alaskan boreal forests, *Ecol. Appl.*, *14*(6), 1826–1838.

Van Cleve, K., L. A. Viereck, and C. T. Dyrness (1996), State factor control of soils and forest succession along the Tanana River in interior Alaska, USA, *Arct. Alp. Res.*, *28*, 388–400.

Viterbo, P., and A. K. Betts (1999), Impact on ECMWF forecasts of changes to the albedo of the boreal forests in the presence of snow, *J. Geophys. Res.*, *104*(D22), 27,803–27,810.

Volney, W. J. A., and R. A. Fleming (2000), Climate change and impacts of boreal forest insects, *Agric. Ecosyst. Environ.*, *82*(1–3), 283–294.

Webb, E. K., G. I. Pearman, and R. Leuning (1980), Correction of flux measurements for density effects due to heat and water vapour transfer, *Q. J. R. Meteorol. Soc.*, *106*(447), 85–100.

Wilson, K. B., et al. (2002), Energy balance closure at FLUXNET Sites, *Agric. For. Meteorol.*, *113*(1–4), 223–243.

F. S. Chapin III, Institute of Arctic Biology, University of Alaska Fairbanks, Fairbanks, AK 99775, USA.

J. Lindfors, Division of Geological and Planetary Sciences, California Institute of Technology, Mail Stop 100-23, Pasadena, CA 91125, USA.

H. Liu, Department of Physics, Atmospheric Sciences and General Science, Jackson State University, P.O. Box 17660, Jackson, MS 39217, USA. (heping.liu@jsums.edu)

J. T. Randerson, Department of Earth System Science, 3212 Croul Hall, University of California, Irvine, CA 92697, USA.